J|A|C|S ARTICLES

Published on Web 03/26/2009

Optimized Acetylene/Carbon Dioxide Sorption in a Dynamic Porous Crystal

Jie-Peng Zhang* and Xiao-Ming Chen*

MOE Key Laboratory of Bioinorganic and Synthetic Chemistry, School of Chemistry and Chemical Engineering, Sun Yat-Sen University, Guangzhou 510275, China

Received November 16, 2008; E-mail: zhangjp7@mail.sysu.edu.cn; cxm@mail.sysu.edu.cn

Abstract: The low compression limit of acetylene (C_2H_2) and its similarity to carbon dioxide (CO_2) challenge the development of novel adsorbents. We illustrate in this report that the unique static and dynamic pore characteristics of a metal azolate framework, $[Cu(etz)]_n$ (MAF-2, Hetz = 3,5-diethyl-1,2,4-triazole), can combine to show extraordinary C_2H_2/CO_2 sorption behaviors, which have been elucidated by a combination of gas sorption measurements and single-crystal structure analyses of the sorption complexes of both C_2H_2 and CO_2. As demonstrated by single-crystal X-ray crystallography, C_2H_2/CO_2 hexamers are confined inside the nanocages of MAF-2 in different configurations. The subtle difference between C_2H_2 and CO_2 is magnified by consequent framework dynamics, which produce sigmoid isotherms that are optimized for practical adsorptive applications. Large C_2H_2 uptake (70 $cm^3\ g^{-1}$) and high C_2H_2/CO_2 uptake ratio (3.7) at 298 K, 1 atm as well as facile gas desorption are revealed. Since the C_2H_2 uptake at 298 K, 1 atm is far from saturation (119 $cm^3\ g^{-1}$), MAF-2 permits a usable C_2H_2 storage capacity 20 times higher than its volume or 40 times higher than that of a gas cylinder working between practical limits of 1.0−1.5 atm.

Introduction

The discovery of novel porous materials for acetylene (C_2H_2) adsorption has attracted great attention due to the difficulties in storage and purification of this important gas.[1−5] Although many adsorbents with micropores and strong host−guest interactions can achieve large uptake of the highly reactive C_2H_2,[1−6] very few of them have demonstrated high C_2H_2 selectivity over its counterpart carbon dioxide (CO_2),[1] despite the fact that separation of C_2H_2 and CO_2 is of great industrial significance. Moreover, the characteristic type I and/or hysteretic sorption behaviors of microporous adsorbents impede facile guest desorption (high vacuum or temperature for desorption is inconvenient and energy-consuming), which is fundamental in practical gas storage and separation using either pressure or temperature swing adsorption (PSA or TSA), although it has been rarely realized.[7] This problem is particularly serious for C_2H_2 compared to other gases, due to its low compression limit (<2 atm),[8] leading to a very limited pressure difference for an adsorption−desorption cycle near ambient conditions.

Although C_2H_2 can be stored and delivered conveniently by dissolving in acetone under high pressure (>10 atm), the volatile solvent contamination restricts its use in fine chemical products and electric materials. Practically, pure C_2H_2 cannot be charged over 1.5 atm or discharged below 1.0 atm; thus, gas cylinders provide very limited delivery or usable storage capacity (USC).[8] Microporous solids may strongly adsorb C_2H_2 to give remarkable uptake at room temperature, but the USC (1.0−1.5 atm) is usually very limited since saturation has been almost or already reached at 1.0 atm. Obviously, the performance is always restricted by the knee-shaped isotherms. In contrast, a sigmoid isotherm whose inflection point (indicated by a maximum peak in its derivative) locates in the working pressure region is optimum for practical adsorptive storage applications. Mesopores or large pores, where host−guest interactions are lower than guest−guest interactions (indicated by very low adsorption enthalpy at low uptakes), can produce sigmoid or type V isotherms.[9] However, the behavior of C_2H_2 in such adsorbents is similar to that of the bulk fluid, and its extremely high reactivity should be considered.

While conventional adsorbents can hardly solve these challenges simultaneously, coordination polymers are potential candidates, as their structures and porous functionalities may be readily tailored for a specified task.[10−24] Valuable information

(1) Matsuda, R.; Kitaura, R.; Kitagawa, S.; Kubota, Y.; Belosludov, R. V.; Kobayashi, T. C.; Sakamoto, H.; Chiba, T.; Takata, M.; Kawazoe, Y.; Mita, Y. *Nature (London)* **2005**, *436*, 238–241.
(2) Samsonenko, D. G.; Kim, H.; Sun, Y.; Kim, G.-H.; Lee, H.-S.; Kim, K. *Chem. Asian J.* **2007**, *2*, 484–488.
(3) Lim, S.; Kim, H.; Selvapalam, N.; Kim, K.-J.; Cho, S. J.; Seo, G.; Kim, K. *Angew. Chem., Int. Ed.* **2008**, *47*, 3352–3355.
(4) Tanaka, D.; Higuchi, M.; Horike, S.; Matsuda, R.; Kinoshita, Y.; Yanai, N.; Kitagawa, S. *Chem. Asian J.* **2008**, *3*, 1343–1349.
(5) Thallapally, P. K.; Dobrzańska, L.; Gingrich, T. R.; Wirsig, T. B.; Barbour, L. J.; Atwood, J. L. *Angew. Chem., Int. Ed.* **2006**, *45*, 6506–6509.
(6) Breck, D. W.; Eversole, W. G.; Milton, R. M.; Reed, T. B.; Thomas, T. L. *J. Am. Chem. Soc.* **1956**, *78*, 5963–5971.
(7) Bhatia, S. K.; Myers, A. L. *Langmuir* **2006**, *22*, 1688–1700.
(8) Leeds, F. H.; Butterfield, W. J. A. *Acetylene, the principle of its generation and use*;Charles Griffin: London, 1910.
(9) Millward, A. R.; Yaghi, O. M. *J. Am. Chem. Soc.* **2005**, *127*, 17998–17999.
(10) Moulton, B.; Zaworotko, M. J. *Chem. Rev.* **2001**, *101*, 1629–1658.
(11) Yaghi, O. M.; O'Keeffe, M.; Ockwig, N. W.; Chae, H. K.; Eddaoudi, M.; Kim, J. *Nature (London)* **2003**, *423*, 705–714.
(12) Kitagawa, S.; Kitaura, R.; Noro, S. I. *Angew. Chem., Int. Ed.* **2004**, *43*, 2334–2375.
(13) Kepert, C. J. *Chem. Commun.* **2006**, 695–700.
(14) Mueller, U.; Schubert, M.; Teich, F.; Puetter, H.; Schierle-Arndt, K.; Pastré, J. *J. Mater. Chem.* **2006**, *16*, 626–636.

 10.1021/ja8089872 CCC: $40.75

can be obtained from the determination of the gas-loaded crystal structures,[25−29] though reported examples for C_2H_2 are still scarce and lack concrete structural information, and no combined study of both C_2H_2 and CO_2 has been performed.[1−3,30] Furthermore, the remarkable framework flexibility of coordination polymers may produce gate-opening or stepwise isotherms whose steeply changing sections are at moderate pressures.[31−38] Such a dynamic adsorbent may facilely release the guest without losing the advantages of micropores and strong host−guest interactions that are prerequisite for C_2H_2. Framework flexibility and guest affinity of the adsorbent must cooperate to improve the performance of C_2H_2 storage and C_2H_2/CO_2 separation near ambient conditions, although little knowledge has been developed in this aspect.

We have designed a coordination polymer, $[Cu(etz)]_n$ (MAF-2, Hetz = 3,5-diethyl-1,2,4-triazole), with unique static and dynamic porous characteristics.[38] MAF-2 can be easily synthesized in high yield and is thermally stable up to 300 °C and chemically stable toward air and moisture. MAF-2 consists of a flexible NbO-type cuprous triazolate scaffold and a bcu pore system with large cavities (the NbO cages) interconnected by small, dynamic apertures. Interestingly, due to the presence of ethyl groups, the NbO cage is modified to be a large sphere (d = 7 Å) octahedrally surrounded by six small pockets (opening

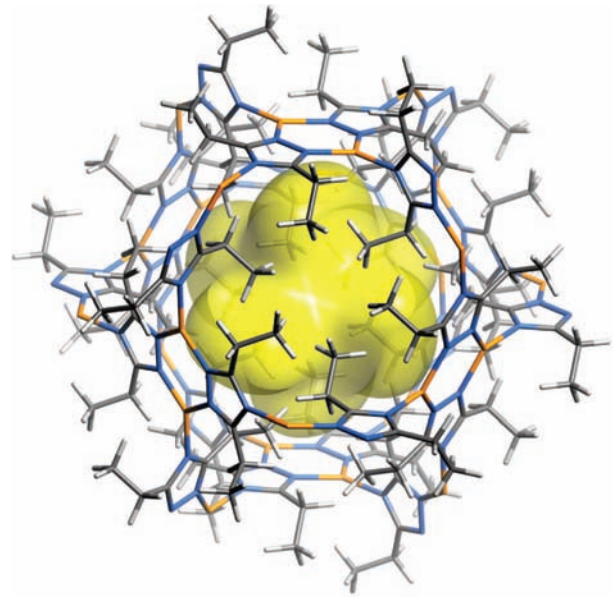

Figure 1. An NbO cage fragment (Cu, orange; N, blue; C, gray; H, white) and the pore surface (yellow) of guest-free MAF-2.

3.4 × 5.4 Å^2, depth 3.4 Å), showing mostly electronegative bottoms (triazolato ring) and electropositive walls (hydrogen atoms of ethyl groups) (Figure 1). These well-defined pockets, which resemble the cleft or crevice of protein surfaces, should stabilize small molecules well and distinguish the size-similar C_2H_2 (3.4 × 3.4 × 5.5 Å^3) and CO_2 (3.4 × 3.4 × 5.3 Å^3) by their opposite quadrupole moments. Moreover, the integration of framework flexibility would be beneficial for novel sorption behaviors. These hypotheses have been corroborated by a combined study of gas sorption measurements and single-crystal X-ray structural analyses.

Experimental Section

Materials and Physical Measurements. Powder and single-crystal samples of MAF-2 were prepared as described previously.[38] Adsorption isotherms were measured by a volumetric adsorption apparatus (Bel-max), with powder samples being degassed under high vacuum at 393 K for 2 h before each measurement; all sorption equilibriums are judged by the same set of criteria. The gas uptake units, cm^3 g^{-1} and cm^3 cm^{-3}, represent cm^3(STP) g^{-1} and cm^3(STP) cm^{-3}, respectively.

X-ray Crystallography. Single crystals of MAF-2 were fixed inside the glass capillaries and pretreated similarly as for the gas adsorption measurements. The capillaries were cooled to room temperature or cryogenic temperature (liquid nitrogen), backfilled with C_2H_2 or CO_2 (5−80 kPa), and finally sealed by a torch. For measurements of saturation adsorption complexes at room temperature, the adsorbate pressures inside the capillaries were 10−20 atm. For other measurements (123 or 195 K, partial or full loading), adsorbate pressures inside the capillaries were controlled by the backfilled pressures. Diffraction intensities were collected on a Bruker Apex CCD area-detector diffractometer (Mo Kα). The structures were solved with direct methods and refined with a full-matrix least-squares technique with the SHELXTL program package. Hydrogen atoms were generated geometrically. For fully loaded structures MAF-2·C_2H_2 and MAF-2·CO_2, anisotropic thermal parameters were applied to all non-hydrogen atoms, while anisotropic thermal parameters were applied to all non-hydrogen atoms of the host framework for partially loaded structures MAF-2·xC_2H_2 and MAF-2·xCO_2 (x = 0.04−0.42). The occupancy x was refined without restraint. The geometries of CO_2 molecules were restrained

(15) Férey, G. *Chem. Soc. Rev.* **2008**, *37*, 191–214.
(16) Morris, R. E.; Wheatley, P. S. *Angew. Chem., Int. Ed.* **2008**, *47*, 4966–4981.
(17) Kosal, M. E.; Chou, J.-H.; Wilson, S. R.; Suslick, K. S. *Nat. Mater.* **2002**, *1*, 118–121.
(18) Lin, X.; Jia, J.-H.; Zhao, X.-B.; Thomas, K. M.; Blake, A. J.; Walker, G. S.; Champness, N. R.; George, M. W.; Hubberstey, P.; Schröder, M. *Angew. Chem., Int. Ed.* **2006**, *45*, 7358–7364.
(19) Pan, L.; Olson, D.-H.; Ciemnolonski, L. R.; Heddy, R.; Li, J. *Angew. Chem., Int. Ed.* **2006**, *45*, 616–619.
(20) Huang, X.-C.; Lin, Y.-Y.; Zhang, J.-P.; Chen, X.-M. *Angew. Chem., Int. Ed.* **2006**, *45*, 1557–1559.
(21) Mulfort, K. L.; Hupp, J. T. *J. Am. Chem. Soc.* **2007**, *129*, 9604–9605.
(22) Ma, S.; Sun, D.; Simmons, J. M.; Collier, C. D.; Yuan, D.; Zhou, H.-C. *J. Am. Chem. Soc.* **2008**, *130*, 1012–1016.
(23) Alkordi, M. H.; Liu, Y.; Larsen, R. W.; Eubank, J. F.; Eddaoudi, M. *J. Am. Chem. Soc.* **2008**, *130*, 12639–12641.
(24) Wu, C.-D.; Hu, A.; Zhang, L.; Lin, W.-B. *J. Am. Chem. Soc.* **2005**, *127*, 8940–8941.
(25) Kawano, M.; Fujita, M. *Coord. Chem. Rev.* **2007**, *251*, 2592–2606.
(26) Serre, C.; Mellot-Draznieks, C.; Surblé, S.; Audebrand, N.; Filinchuk, Y.; Férey, G. *Science* **2007**, *315*, 1828–1831.
(27) Dincă, M.; Han, W. S.; Liu, Y.; Dailly, A.; Brown, C. M.; Long, J. R. *Angew. Chem., Int. Ed.* **2007**, *46*, 1419–1422.
(28) Rowsell, J. L. C.; Spencer, E. C.; Eckert, J.; Howard, J. A. K.; Yaghi, O. M. *Science* **2005**, *309*, 1350–1354.
(29) (a) Takamizawa, S.; Nakata, E.-I.; Yokoyama, H.; Mochizuki, K.; Mori, W. *Angew. Chem., Int. Ed.* **2003**, *42*, 4331–4334. (b) Takamizawa, S.; Nakata, E.-I.; Akatsuka, T. *Angew. Chem., Int. Ed.* **2006**, *45*, 2216–2221. (c) Takamizawa, S.; Kohbara, M.-A. *Dalton Trans.* **2007**, *42*, 3640–3645.
(30) Kubota, Y.; Takata, M.; Matsuda, R.; Kitaura, R.; Kitagawa, S.; Kobayashi, T. C. *Angew. Chem., Int. Ed.* **2006**, *45*, 4932–4936.
(31) Kitaura, R.; Seki, K.; Akiyama, G.; Kitagawa, S. *Angew. Chem., Int. Ed.* **2003**, *42*, 428–431.
(32) Lee, E. Y.; Jang, S. Y.; Suh, M. P. *J. Am. Chem. Soc.* **2005**, *127*, 6374–6381.
(33) Zhang, J.-P.; Lin, Y.-Y.; Zhang, W.-X.; Chen, X.-M. *J. Am. Chem. Soc.* **2005**, *127*, 14162–14163.
(34) Maji, T. K.; Matsuda, R.; Kitagawa, S. *Nat. Mater.* **2007**, *6*, 142–148.
(35) Bradshaw, D.; Warren, J. E.; Rosseinsky, M. J. *Science* **2007**, *315*, 977–980.
(36) Chandler, B. D.; Enright, G. D.; Udachin, K. A.; Pawsey, S.; Ripmeester, J. A.; Cramb, D. T.; Shimizu, G. K. H. *Nat. Mater.* **2008**, *7*, 229–235.
(37) Horike, S.; Matsuda, R.; Tanaka, D.; Matsubara, S.; Mizuno, M.; Endo, K.; Kitagawa, S. *Angew. Chem., Int. Ed.* **2006**, *45*, 7226–7230.
(38) Zhang, J.-P.; Chen, X.-M. *J. Am. Chem. Soc.* **2008**, *130*, 6010–6017.

Table 1. Crystallographic Data and Refinement Parameters of Gas-Free and -Loaded MAF-2[a]

	MAF-2	MAF-2·0.5N_2	MAF-2·C_2H_2	MAF-2·C_2H_2	MAF-2·CO_2
formula	$C_6H_{10}CuN_3$	$C_6H_{10}CuN_4$	$C_8H_{12}CuN_3$	$C_8H_{12}CuN_3$	$C_7H_{10}CuN_3O_2$
FW	187.71	188	213.75	213.75	231.72
space group	$R\bar{3}$	$R\bar{3}$	$R\bar{3}$	$R\bar{3}$	$R\bar{3}$
T/K	123(2)	93(2)	123(2)	293(2)	123(2)
a/Å	19.6891(8)	19.6052(5)	19.5289(8)	19.6972(9)	19.6216(12)
c/Å	14.1971(7)	14.2420(4)	14.2935(8)	14.2478(8)	14.2113(9)
V/Å^3	4766.3(4)	4740.7(2)	4720.9(4)	4787.3(4)	4738.4(5)
Z	18	18	18	18	18
D_c/g cm^{-3}	1.177	1.272	1.353	1.335	1.360
μ/mm^{-1}	2.007	2.025	2.035	2.007	2.042
restraints	0	1	0	0	2
R_1 ($I > 2\sigma$)	0.0402	0.0327	0.0393	0.0510	0.0458
wR_2 (all data)	0.0770	0.0761	0.0820	0.1182	0.1004
GOF	1.014	1.015	1.028	1.021	1.057

[a] $R_1 = \sum||F_o| - |F_c||/\sum|F_o|$, $wR_2 = [\sum w(F_o^2 - F_c^2)^2/\sum w(F_o^2)^2]^{1/2}$.

(Tables 1 and S2 in the Supporting Information). Structures of MAF-2 and MAF-2·0.5N_2 measured at 123(2) K have been reported in ref 38.

Results and Discussion

Sorption Properties. C_2H_2/CO_2 sorption isotherms were measured at 195, 273, and 298 K (Figure 2). Except for CO_2 at 298 K, the isotherms are apparently sigmoidal, which can be clearly identified from the presence of an inflection point in the derivative of the isotherm (Figures S1−S6, Supporting Information). The 195 K isotherms seem like type I, as their inflection points locate at very low pressures. Their saturation uptakes, ca. 119 cm^3 g^{-1}, correspond to one C_2H_2/CO_2 per pocket or six per NbO cage, indicating stoichiometric recognition. A large C_2H_2/CO_2 uptake ratio of 30 was observed at 70 Pa, but the temperature and pressure are too low for practical interest (Figure S7, Supporting Information). At 298 K, 1 atm, the C_2H_2 uptake of 70 cm^3 g^{-1} (82 cm^3 cm^{-3}) represents a high value among various adsorbents and is just lower than those of zeolite 4A (98 cm^3 g^{-1}, 150 cm^3 cm^{-3})[6] and several coordination polymers (82−106 cm^3 g^{-1}, 77−116 cm^3 cm^{-3}) with relatively large pore volumes.[4] In contrast to the monotonic (Langmuir, type I) and/or hysteretic isotherms resulting from micropores and strong host−guest interactions, the sigmoidal, fully reversible C_2H_2 isotherm of MAF-2 at 298 K would permit not only large adsorption at 1 atm but also facile desorption at moderately low pressures. Among six measured isotherms, hystereses are observed only for the 273 (very small) and 195 K C_2H_2 isotherms, indicating good sorption reversibility, especially at room temperature, in the seemingly impermeable MAF-2.[39,40] The observed diffusion differences should be ascribed to the temperature-dependent ethyl motion[38] and formation of different adsorbed states for C_2H_2 and CO_2.

The 298 K C_2H_2 isotherm of MAF-2 has a large positive slope at 1.0 atm, indicating more C_2H_2 uptake at higher pressures. On the basis of the information obtained from the low-temperature isotherms (Figure S8, Supporting Information), we extrapolated the 298 K isotherm to 1.5 atm. The estimated C_2H_2 uptake at 1.5 atm is 87 cm^3 g^{-1} (102 cm^3 cm^{-3}), corresponding to a 17 cm^3 g^{-1} (20 cm^3 cm^{-3}) difference from that at 1.0 atm. In other words, one volume of MAF-2 at room temperature, working between 1.0 and 1.5 atm, can deliver 21 volumes of C_2H_2 (volume at 298 K), which is 40 times higher than that of a gas cylinder. In this context, MAF-2 also outperforms acetone

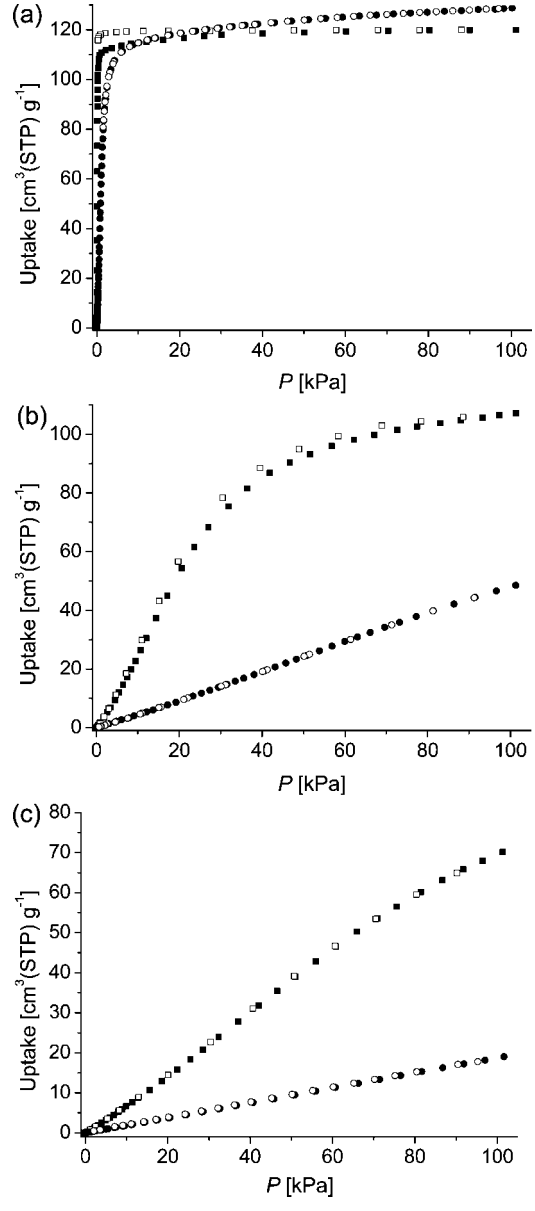

Figure 2. Sorption isotherms of C_2H_2 (squares) and CO_2 (circles) for MAF-2 at 195 (a), 273 (b), and 298 K (c). The filled and open symbols represent adsorption and desorption, respectively.

(39) Zhao, X.; Xiao, B.; Fletcher, A. J.; Thomas, K. M.; Bradshaw, D.; Rosseinsky, M. J *Science* **2004**, *306*, 1012–1015.
(40) Thallapally, P. K.; McGrail, B. P.; Dalgarno, S. J.; Schaef, H. T.; Tian, J.; Atwood, J. L. *Nat. Mater.* **2008**, *7*, 146–150.

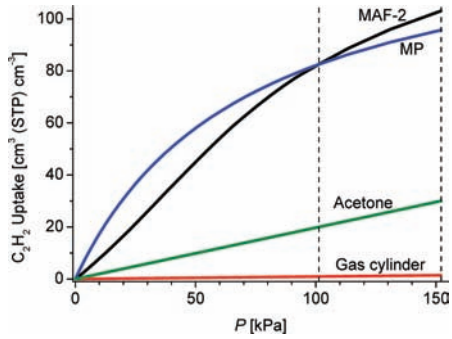

Figure 3. Volumetric C_2H_2 uptakes of MAF-2 and other typical materials at room temperature. Two dashed lines represent the practical working limit of charging and discharging pressures. MP is a hypothetical microporous adsorbent (follows Langmuir isotherm) having the same uptake as MAF-2 at both 1 atm and P_0.

and its "Langmuir analogue" (Figure 3), as well as other typical microporous adsorbents.

Also remarkably, the CO_2 uptake at 298 K, 1 atm was significantly reduced to 19 cm^3 g^{-1}. The C_2H_2/CO_2 uptake ratio of 3.7 at 298 K, 1 atm is much higher than those of other adsorbents (1.0−1.7), although they may increase at lower pressures according to the knee-shaped isotherms.[1−6] The exceptional C_2H_2/CO_2 sorption behaviors of MAF-2 would allow PSA purification to be performed at near-ambient conditions, which is beneficial for practical applications. The CO_2 uptake of MAF-2 at 273 K, 1 atm is still 49 cm^3 g^{-1} and has a large slope, indicating a moderate CO_2 affinity.[41] The easily altered CO_2 uptake upon changing temperature and/or pressure indicates that MAF-2 could be a good CO_2 reservoir. Instead of moderate CO_2 affinity, the lack of an inflection point in the 298 K isotherm rules out significant uptake below 1 atm. The disappearance of a sigmoid isotherm may be ascribed to the pressure limit of the measurement, as the inflection point could locate at higher than 1 atm. By comparing the six measured isotherms, it is evident that factors such as framework flexibility, which induce a sigmoid isotherm, become less important at higher temperatures for weaker adsorbing guest.

Adsorption isosteric heats (q_{st}) were calculated by using the Clausius−Clapeyron equation to produce a clearer map of adsorption mechanism. The obtained q_{st} values lie in the ranges of 29.8−33.7 and 25.8−26.9 kJ mol^{-1} for C_2H_2 and CO_2, respectively (Figure S8). The q_{st} difference (4.0−6.7 kJ mol^{-1}) between C_2H_2 and CO_2 represents a moderate difference in host−guest binding affinity. The C_2H_2 q_{st} of MAF-2 is moderate among the reported values (27−59 kJ mol^{-1}) for microporous adsorbents.[1−4] By the aid of crystallography, the highest C_2H_2 q_{st} values observed in cucurbit[6]uril (59.4 kJ mol^{-1})[3] and $[Cu_2(pzdc)_2(pyz)]_n$ (42.5 kJ mol^{-1}; pzdc = pyrazine-2,3-dicarboxylate, pyz = pyrazine)[1] were attributed to the strong C−H···O hydrogen-bonding between C_2H_2 and oxygen of the host. $[M_2(bdc)_2(dabco)]_n$ (M = Cu^{2+}/Zn^{2+}, bdc = 1,4-benzenedicarboxylate, dabco = 1,4-diazabicyclo[2.2.2]octane)[42,43] showed sigmoid isotherms with high C_2H_2 uptakes (60/93 cm^3 g^{-1}, 49/77 cm^3 cm^{-3} at 298 K, 1 atm).[4] However, their exceptionally low q_{st} values (20.6−24.0 kJ mol^{-1}) indicate that C_2H_2 is very labile in the relatively large pores (d = 10 Å, aperture 7.5 × 7.5 Å^2). Interestingly, during the adsorption processes, the C_2H_2 q_{st} first decreases from low uptake (33.3 kJ mol^{-1} at 1 cm^3 g^{-1}) to a minimum (29.8 kJ mol^{-1} at 7 cm^3 g^{-1}), and then slightly increases until a high uptake (33.7 kJ mol^{-1} at 70 cm^3 g^{-1}). The q_{st} trend of CO_2 is similar but less remarkable (26.6, 25.8, and 26.9 kJ mol^{-1} at 1, 7, and 49 cm^3 g^{-1}, respectively). The q_{st} change profiles are in accordance with the sigmoid isotherms, but the origin of these changes deserves detailed analysis.

For conventional adsorbents, the initial decrease of q_{st} can be attributed to the presence of heterogeneity (different binding sites),[44,45] while subsequent increases of q_{st} can originate from the increasing contribution of guest−guest interactions (for large pore and guest−guest interaction > host−guest interaction).[4,9] These q_{st} changes can be also a consequence of structural transformation of the adsorbent. As revealed by the stoichiometric adsorption of N_2, MeOH, EtOH, and MeCN and corresponding crystallographic studies, MAF-2 contains only one type of adsorption site, as its pore surface pocket can accommodate only one guest molecule.[38] The guest−guest interaction can be significant for solvents, which interact with MAF-2 via van der Waals forces but with each other via strong hydrogen bonds. Nevertheless, even weak host−guest interactions can induce noticeable framework distortions to the flexible scaffold of MAF-2. Therefore, the q_{st} changes could be tentatively assigned to the structural transformation of MAF-2, in which the stronger host−guest interaction induces the larger q_{st} change ($C_2H_2 > CO_2$), though guest−guest interactions may also have some contribution. The answer to how C_2H_2/CO_2 interact with MAF-2 and with each other is connected to the sorption mechanism and the reactivity of the adsorbed C_2H_2.

Structural Insight. Direct structural information about the sorption complexes is fundamental to the understanding of the sorption mechanism and rational design of new adsorbents. However, due to the weak gas-binding ability and/or poor sample crystallinity after guest exchange, the few reports on gas-loaded crystal structures are mainly concerned with ultramicropores and/or synchrotron powder diffraction techniques. Thanks to the good flexibility and robustness of MAF-2, we obtained fine single-crystal structures of the gas sorption complexes MAF-2·C_2H_2 and MAF-2·CO_2. Compared with the guest-free MAF-2, anisotropic unit-cell distortions are evident (at 123 K) for MAF-2·C_2H_2 ($\Delta a/c$ = −1.5%, ΔV = −1.0%) and MAF-2·CO_2 ($\Delta a/c$ = −0.4%, ΔV = −0.6%), which revealed small but non-negligible framework deformations. We have also shown that inclusion of weakly adsorbing N_2 cannot produce noticeable framework deformations for MAF-2 (Table 1).[38] Although it is difficult to obtain precise energy profiles,[46,47] the small deformation in MAF-2·C_2H_2 may consume energy up to several kJ mol^{-1}, whereas this value should be substantially lower for MAF-2·CO_2. For reference, a small expansion (ΔV = +1.7%) of $[Cu_2(pzdc)_2(pyz)]_n$ increases the framework energy by 6.8 kJ mol^{-1}.[1] Therefore, the initial q_{st} decreases upon C_2H_2/CO_2 uptake correlate well with the framework flexibility of MAF-2.

(41) Wang, B.; Côté, A. P.; Furukawa, H.; O'Keeffe, M.; Yaghi, O. M. *Nature (London)* **2008**, *453*, 207–211.
(42) Seki, K.; Mori, W. *J. Phys. Chem. B* **2002**, *106*, 1380–1385.
(43) Dybtsev, D. N.; Chun, H.; Kim, K. *Angew. Chem., Int. Ed.* **2004**, *43*, 5033–5036.
(44) Forster, P. M.; Eckert, J.; Chang, J.-S.; Park, S.-E.; Férey, G.; Cheetham, A. K. *J. Am. Chem. Soc.* **2006**, *128*, 16846–16850.
(45) Chen, B.; Zhao, X.; Putkham, A.; Hong, K.; Lobkovsky, E. B.; Hurtado, E. J.; Fletcher, A. J.; Thomas, K. M. *J. Am. Chem. Soc.* **2008**, *130*, 6411–6423.
(46) Choi, H. J.; Dincă, M.; Long, J. R. *J. Am. Chem. Soc.* **2008**, *130*, 7848–7850.
(47) Coudert, F.-X.; Jeffroy, M.; Fuchs, A. H.; Boutin, A.; Mellot-Draznieks, C. *J. Am. Chem. Soc.* **2008**, *130*, 14294–14302.

In addition to the thermodynamically controlled flexibility (TCF) and framework distortion between equilibrium states,[31−36] kinetically controlled flexibility (KCF) is a more pronounced feature of MAF-2, in which temporary ethyl motions allow guest diffusion through the seemingly impermeable framework without permanent structural transformation. This kind of framework flexibility is useful for a temperature-controlled gate-opening function.[38] Aside from the small deformations, the host framework remains essentially unchanged, and the NbO cages are still separated from each other after inclusion of C_2H_2/CO_2, confirming the occurrence of KCF or temporary ethyl motions. In principle, the zero-dimensional pores could prevent the propagation of C_2H_2 decomposition/polymerization, if present.

Because the ethyl motion depends not only on temperature but also on guest molecules, it may also affect the adsorption energy. At the guest-free state, ethyl groups have the highest degree of freedom and maximum available free volume, accompanying relatively large thermal motion and high framework energy. By introducing steric hindrance, uptake of guest reduces ethyl motion and decreases framework energy. The energy difference depends on the efficiency of guest in interrupting the framework motion. For example, the equilibrium static and dynamic states of $[Zn_2(ndc)_2(dabco)]_n$, having an enthalpy difference of 4.32 kJ mol^{-1}, can be switched by adsorption/desorption of benzene.[37] Comparing the thermal parameters of the gas-free and -adsorbed phases revealed significant reduction of thermal motions on the terminal methyl groups of etz upon C_2H_2 uptake, but the effect of CO_2 was negligible, indicating that C_2H_2 gains more stabilizing energy than CO_2 from the KCF (Figure S9 and Table S1, Supporting Information). The energetic effect of KCF is compatible to those of permanent framework transformations and guest−guest interactions. These effects may combine to develop the sigmoid isotherms and magnify the difference between different guests. Nevertheless, due to the lack of adequate information on these very complicated, extended systems, it is difficult to deconvolute the exact energy contribution of each effect from the present data.

Besides the framework atoms, only one C_2H_2/CO_2 was revealed for each formula unit [Cu(etz)], matching well with the adsorption data. Although the diffractions were just measured by laboratory X-ray at 123 K, the structure of C_2H_2, including bonding distance (1.146(9) Å) and anisotropic thermal parameters, can be refined without restraint, providing the most accurate structural information so far. Actually, only a few C_2H_2-adsorbed ultramicroporous molecular adsorbents have been crystallographically determined by the aid of low-temperature, synchrotron radiation, and/or powder diffraction techniques.[1−3,30] A reliable crystal structure of MAF-2·C_2H_2 without apparent disorder can be determined even at room temperature, indicating that C_2H_2 is strongly fixed. In contrast, to refine the structure of MAF-2·CO_2 at 123 K, soft restraints for the C−O distances (1.16(1) Å) are required, and the CO_2 cannot be modeled at higher temperatures. Some C_2H_2-adsorbed zeolites have been studied by single-crystal X-ray diffraction at room temperature, but the C_2H_2 molecules are seriously disordered.[48]

Being confined in the octahedral cage, the molecular axis of C_2H_2 points toward the pocket bottom plane with an inclination angle 27.7° (Figure 4a). The strongest host−guest interactions are C−H···N contacts (C···N = 3.44 and 3.47 Å, H···N = 2.61 and 2.50 Å) between C_2H_2 and the 1,2-nitrogens of etz, which represent the most electronegative part of MAF-2. The long C−H···Cu separation (C···Cu = 4.29 Å, H···Cu = 3.25 Å) indicates that C_2H_2 is not likely interacting with the metal ions. As the pocket is not deep enough, part of the C_2H_2 resides outside the pocket. Consequently, the outer ends of six C_2H_2 molecules interact with each other by C−H···C contacts (C···C = 3.69 Å, H···C = 2.69 Å) in a T-shaped conformation to form an unprecedented, S_6 cyclic hexamer (Figure 4b). The relatively long C−H···C contacts and large thermal parameters of the outer carbon atom indicate substantially weaker guest−guest interactions compared with the host−guest ones. The unique cage shape and surface characteristic ensure that C_2H_2 molecules are confined in a configuration that allows large uptake and prevents reactive contacts inside the large cavity.

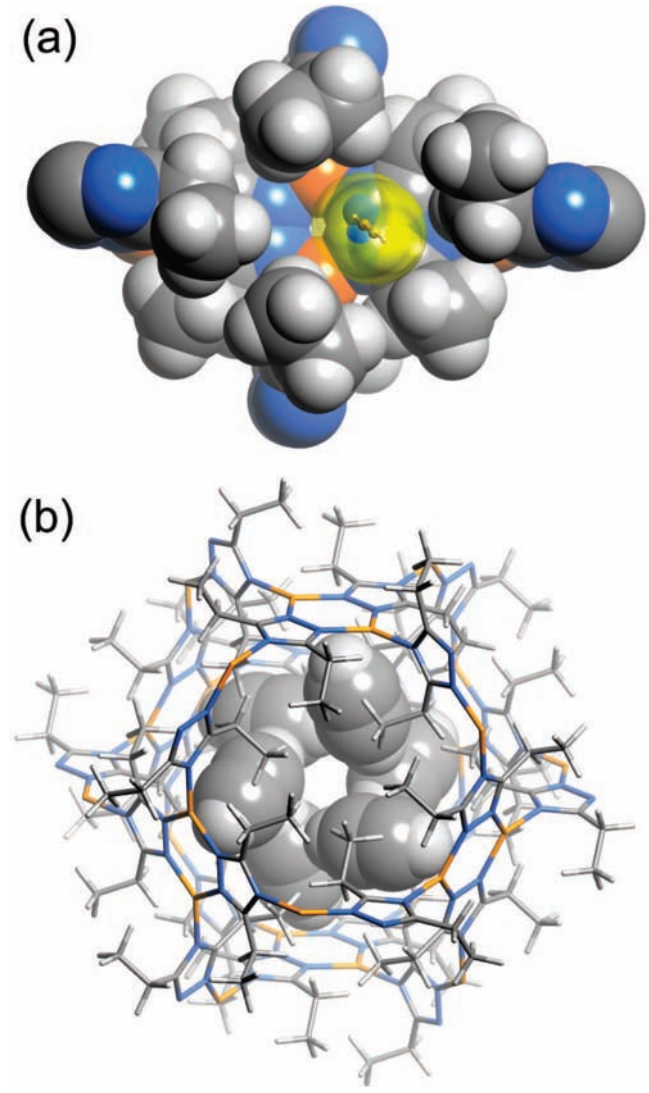

Figure 4. A C_2H_2 molecule inside the pocket (a) and the hexameric arrangement of C_2H_2 molecules within the cage (b) of MAF-2.

In MAF-2·CO_2, CO_2 is well embedded inside the pocket (inclination angle 89.8°) and forms short contacts with the 1,2-nitrogens of etz by its electropositive carbon (C···N = 3.40/3.41 Å) (Figure 5a). Compared to the oxygens, the relatively small thermal motion of this carbon indicates the predominance of this interaction. Inside the cage, CO_2 molecules are well separated (C···O = 4.58 Å) around a void (d = 4 Å), indicating weak guest−guest interaction and loose structure (Figure 5b).

(48) Jang, S. B.; Jeong, M. S.; Kim, Y.; Seff, K. *J. Phys. Chem. B* **1997**, *101*, 3091–3096.

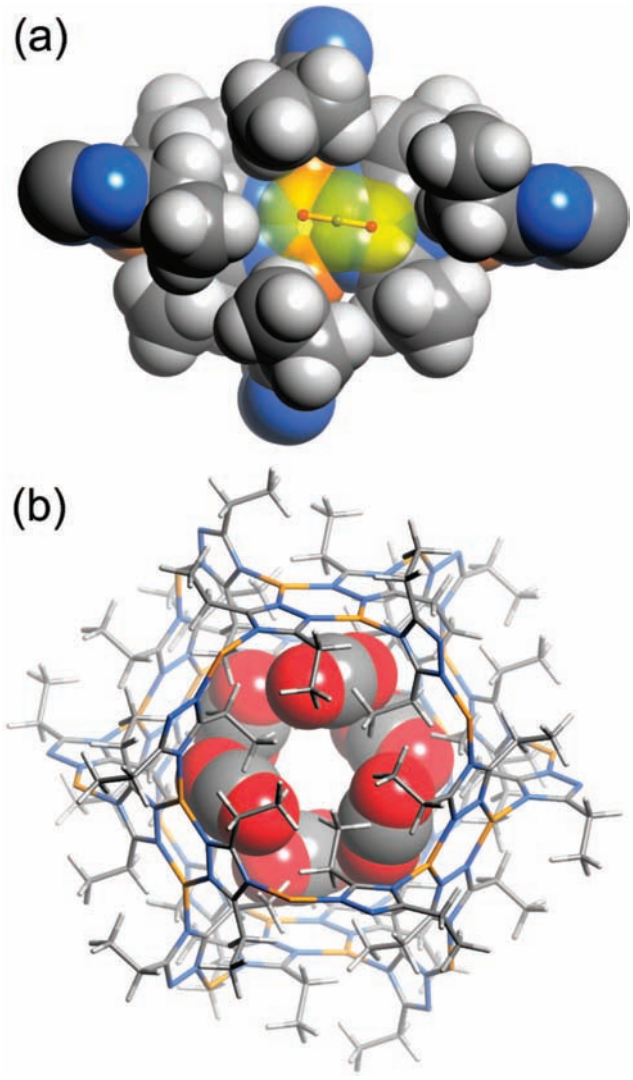

Figure 5. A CO_2 molecule inside the pocket (a) and six CO_2 molecules within the cage (b) of MAF-2.

The electron-rich nitrogen is known to interact with CO_2 and play an important role in the adsorption,[9] but direct structural evidence has not been reported yet. The coordinated nitrogens of MAF-2 are likely not providing lone pairs but just serving as electronegative sites. Obviously, a simple hydrogen-bonding acceptor does not distinguish C_2H_2 and CO_2 well from the adsorptive point of view, as they can adopt different orientations to achieve maximum interactions, which explains the generally observed low C_2H_2/CO_2 uptake ratios. Inside MAF-2, an oxygen of CO_2 also has to lie above the electronegative triazolato ring, which reduces the CO_2 binding enthalpy. Nevertheless, the CO_2 binding enthalpy should not be significantly lower than that of C_2H_2, as the pocket wall fits CO_2 well with multiple C−H···O interactions (C···O = 3.31−3.47 Å).

The gas-adsorbed structures confirmed that C_2H_2 and CO_2 bind to the well-defined pore surface very differently. Similar to the binding of guests on the cleft or crevice of protein surfaces, gas molecules on the pore surface of MAF-2 are stabilized by cooperation of multiple weak supramolecular interactions. The unique pore surface and confined cages combine the advantages of both small and large pores, which strongly restrict large amounts of C_2H_2 in a safe packing configuration.

To obtain more information during the whole adsorption processes, we have also measured the partial loading crystal structures by varying the temperature and adsorbate pressure in a wide range. However, the crystallographic data obtained for MAF-2·$x$$C_2H_2$ and MAF-2·$x$$CO_2$ ($0 < x < 1$) degrade from those of the fully loading structures, especially when temperature is high and/or x is small, which is common in crystallographic studies of host−guest systems. Nevertheless, a series of comparable data sets were obtained at 195 K and $0.04 < x < 0.42$. For comparison, the crystal structure of guest-free MAF-2 was also measured at the same temperature. It seems that the framework deformations were started from very low loadings and almost completed at $x \approx 0.2$. The thermal parameters of framework atoms also decrease as uptake increase (from $x = 0.04$ to $x = 0.42$). These observations are in accordance with the observed q_{st} changes. On the other hand, the locations of gas molecules in these structures can be regarded to be unaltered (Figure S10) in the accuracy range of experiment (only occupancies increase), which confirm that there is no observable structural rearrangement of guest or differential adsorption site.

Conclusion

According to the sorption measurements and crystallographic analyses, we may conclude that the sigmoid isotherms of MAF-2 do not likely originate from the structural rearrangement of guest or the presence of differential adsorption sites (heterogeneity). Although the host structure is seemingly impermeable, the highly flexible ethyl groups would allow the gas to diffuse into the pores even at extremely low adsorbate pressures. Only when the temperature is extremely low (e.g., 77 K) or the guest (e.g., water) is incompatible with the hydrophobic apertures would MAF-2 behave as a nonporous material. The gas molecules should first enter the pores and then induce framework deformations (TCF) and restrict framework motions (KCF). Therefore, the sigmoid isotherm can be assigned to the framework dynamics of MAF-2. The formation of supramolecular clusters of gas molecules may also contribute to the sigmoid isotherm by introducing guest−guest interaction energy. Nevertheless, this energy should be very low, as judged from the hexamer configurations.

Although the adsorption energy difference between C_2H_2 and CO_2 is not large enough for a good adsorptive separation, the performance is magnified by cooperation of dynamic responses of the flexible framework, which are seemingly trivial but indeed influence the whole sorption processes by extracting or adding energy from/to the host−guest system. The resulting energy profiles and accompanying sigmoid sorption isotherms are optimized for practical adsorptive applications. These results should demonstrate new directions for the design, characterization, and application of new adsorbents.

Acknowledgment. This work was supported by the "973 Program" (2007CB815302), NSFC (No. 20821001 and 20531070), and Sun Yat-Sen University.

Supporting Information Available: Crystallographic data (CIF); additional structural plots and tables (PDF). This material is available free of charge via the Internet at http://pubs.acs.org.

JA8089872